# Deviation from Arrhenius behaviour of rate of intercage diffusion in Zeolite Y[1]

PRAKRITESWAR SANTIKARY† AND SUBRAMANIAN YASHONATH‡

†*Solid State and Structural Chemistry Unit*
‡*Supercomputer Education and Research Centre, Indian Institute of Science, Bangalore-560012, India*

SUMMARY

Rate of intercage diffusion ($k_c$) along with rate of cage visits ($k_v$) and diffusion coefficient ($D$) of sorbates in zeolite Y have been calculated. We show that as a consequence of the dependence of rate of intercage diffusion on short-time behaviour, significant deviation from the Arrhenius behaviour at suffciently high temperatures occurs.

KEY WORDS diffusion; Arrhenius law; zeolite Y; molecular dynamics

## 1. INTRODUCTION

A number of results on zeolite Y obtained from molecular dynamics (MD) simulations have been analysed by calculating three important properties, namely, the rate of intercage diffusion, $k_c$, the rate of cage visits, $k_v$ and the diffusion coefficient, $D$ [1–3]. Calculations on xenon sorbed in zeolite NaY indicate that the slope obtained from the Arrhenius plot of the rate of intercage diffusion leads to an activation energy of about 3.02 kJ mol$^{-1}$ [1]. In zeolite NaCaA $k_c$ shows a peculiar behaviour: below 500 K, the slope of the Arrhenius plot of $k_c$ suggests a negative activation energy of $-0.95$ kJ mol$^{-1}$. Above 500 K the activation energy was found to be positive with $E_a$ = 1.38 kJ mol$^{-1}$ [3]. These surprising results were interpreted in terms of the underlying potential energy surface and the surface-mediated (s.-m.) and centralized diffusion (c.d.) mechanisms. It was suggested that the rate of intercage diffusion depends on the short-time behaviour. It was also suggested that properties such as $k_v$ and $D$ depend on the long-time behaviour of the system. In order to see if $k_c$ depends on the short-time behaviour and $k_v$ and D on the long-time behaviour we report here long MD simulations of xenon sorbed in zeolite NaY over a large range of temperatures. $k_c$, $k_v$ and $D$ and their temperature dependence have been calculated to see if the Arrhenius behaviour is satisfied by these three properties.

## 2. STRUCTURE OF ZEOLITE Y

The structure of zeolite Y was taken from the recent neutron diffraction study of Fitch *et al.* [4]. The structure is similar to that reported by Olson [5]. The lattice parameter of the bare zeolite at room temperature with $a$ = 24.8536 Å has been employed. The space group is Fd$\bar{3}$m. The unit cell formula is $Na_{48}Si_{144}Al_{48}O_{384}$ for a Si/Al ratio of 3.0. For this particular ratio the extra framework sodium

[1] Contribution No. 1104 from the Solid State and Structural Chemistry Unit.

Table 1. Interatomic potential parameters for sorbate–sorbate and sorbate–zeolite interactions

| Atom | $\epsilon$ (K) | $\sigma$ (Å) |
|---|---|---|
| Sorbate–sorbate | | |
| Xe–Xe | 221.0 | 4.1 |
| Sorbate–zeolite | | |
| Xe–O | 185.1 | 3.32 |
| Xe–Na | 32.3 | 3.74 |

ions occupy $S_{\mathrm{I}}$ and $S_{\mathrm{II}}$ sites completely [6]. Zeolite Y structure consists of sodalite and supercages or $\alpha$-cages. The sodalite cages are small with an approximate diameter of 4.4 Å and therefore no Xe atoms are found to adsorb in these cages. The $\alpha$-cage diameter is $\sim$11.8 Å and therefore Xe atoms are found to adsorb in these cages. There are eight such $\alpha$-cages in one unit cell. Each $\alpha$-cage is tetrahedrally connected to four other $\alpha$-cages through the 12-ring window of approximate diameter 8 Å. The window is made up of 12 Si/Al and 12 O atoms. Below we use cage and $\alpha$-cage interchangeably.

## 3. INTERMOLECULAR POTENTIAL FUNCTIONS

### 3.1. Sorbate–sorbate interactions

Sorbate–sorbate interactions have been modelled in terms of (6–12) Lennard–Jones pair potential

$$\phi_{\mathrm{ss}}(r_{\mathrm{ss}}) \;=\; 4\epsilon_{\mathrm{ss}}\left[\left(\frac{\sigma_{\mathrm{ss}}}{r_{\mathrm{ss}}}\right)^{12} - \left(\frac{\sigma_{\mathrm{ss}}}{r_{\mathrm{ss}}}\right)^{6}\right] \tag{1}$$

where $s$ stands for sorbate. The $\sigma_{\mathrm{ss}}$ and $\epsilon_{\mathrm{ss}}$ for xenon were taken from literature [7] and are listed in Table 1.

### 3.2. Sorbate–zeolite Interactions

These have been modelled again in terms of short-range (6–12) Lennard–Jones potential

$$\phi_{\mathrm{sz}} = -\frac{A_{\mathrm{sz}}}{r_{\mathrm{sz}}^{6}} + \frac{B_{\mathrm{sz}}}{r_{\mathrm{sz}}^{12}} \tag{2}$$

where $s$ stands for sorbate and z = Si, O and Na. The value of $A_{\mathrm{sz}}$ and $B_{\mathrm{sz}}$ were obtained from the relation $\mathrm{A_{sz}} = 4\epsilon_{\mathrm{sz}}\sigma_{\mathrm{sz}}^{6}$ and $\mathrm{B_{sz}} = 4\epsilon_{\mathrm{sz}}\sigma_{\mathrm{sz}}^{12}$. The potential depth $\epsilon_{\mathrm{sz}}$ and the diameter $\sigma_{\mathrm{sz}}$ were calculated from the Lorentz–Berthelot combination rules [7]

$$\epsilon_{\mathrm{sz}} = (\epsilon_{\mathrm{ss}}\epsilon_{zz})^{1/2} \tag{3a}$$

$$\sigma_{\mathrm{sz}} = (\sigma_{\mathrm{ss}} + \sigma_{zz})/2 \tag{3b}$$

The values of $\epsilon_{zz}$ and $\sigma_{zz}$ were obtained from the work of Kiselev and Du [8]. The sigma and epsilon values for the sorbate–sorbate and sorbate–zeolite atoms are listed in Table 1.

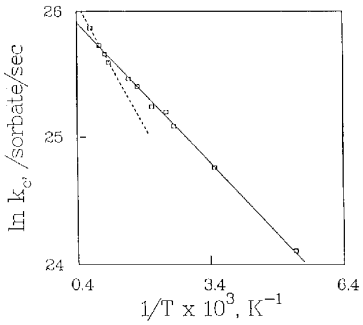


*Figure 1. Arrhenius plot of $k_c$. The straight line fitted to the lowest seven temperatures is shown by means of a continuous line; the line fitted to the highest four temperatures is shown by means of a broken line*

## 4. COMPUTATIONAL DETAILS

All calculations were carried out in the microcanonical ensemble at fixed $N$, $V$ and $E$. One unit cell of zeolite NaY has been used. Cubic periodic conditions were employed. MD integration was carried out by using well-known Verlet algorithm [7]. The zeolite atoms were assumed to be rigid and were not included in the MD integration. Interaction between sorbate and Si atoms was taken to be zero. This is because each silicon atom is surrounded by bulkier oxygen atoms and thereby prevents the sorbate atom from coming in close to silicon atoms. Another assumption made in the present calculations is the neglect of polarizability interactions between xenon and the zeolite atoms. This is expected to contribute not more than 15% to the total interactions. A cut-off radius of 12 Å was used for the calculations of both sorbate–sorbate and sorbate–zeolite interaction energies and forces. Calculations were performed at eleven different temperatures, namely, 188, 285, 386, 414, 425, 479, 567, 637, 897, 970, 1107 and 1420 K at a sorbate loading of 1 Xe/$\alpha$-cage. A time step of 40 fs was found to yield good energy and momentum conservation for the first six temperatures while 10 fs was used for the last five temperatures. Equilibration was carried out over a period of 250 ps during which velocities were scaled at each step to obtain the desired temperature. Long production runs of 2600 ps were performed at each temperature. Long simulation runs were required to obtain reasonable statistics of the dynamical properties of our interest. Properties were calculated from configurations stored at intervals of 0.2 ps. The xenon mass was taken as 131 amu.

The method employed by us for the calculation of $k_c$ and $k_v$ is straightforward. The cage in which a particular sorbate atom is resident at a given time step is found by calculating the distance between all the cage centres and the sorbate. The resident cage is that cage whose sorbate–cage centre distance is the shortest. The instant at which the sorbate has diffused to a neighbouring cage is taken to be the time step when the resident cage is different from that of the previous time step. At this instant the perpendicular distance between the sorbate and the plane of the 12-ring window is nearly zero. For the calculation of the rate of intercage diffusion, the number of diffusions from one cage to another is noted during the course of the simulation. The rate of cage visits is obtained from the rate of intercage diffusion by eliminating all the diffusion events from cage i to j which are either followed or preceded by diffusion from cage j to i. More details are discussed in the earlier work on zeolite Y [1]. The diffusion coefficient is obtained from the long-time slope of the mean square displacement versus time plot [7].

Table 2. Rate of intercage diffusion, $k_c$, rate of cage visits, $k_v$ and the diffusion coefficient, $D$ for xenon in NaY at different temperatures

| $T$ (K) | $k_c \times 10^{-10}$ (sorbate$^{-1}$s$^{-1}$) | $k_v \times 10^{-10}$ (sorbate$^{-1}$s$^{-1}$) | D$\times 10^8$ (m$^2$ s$^{-1}$) |
|---|---|---|---|
| 188 | 24.10 | 23.38 | 0.29 |
| 285 | 24.76 | 24.23 | 0.77 |
| 386 | 25.08 | 24.59 | 1.28 |
| 414 | 25.20 | 24.72 | 1.30 |
| 479 | 25.24 | 24.91 | 1.43 |
| 567 | 25.40 | 25.10 | 1.82 |
| 637 | 25.46 | 25.12 | 1.87 |
| 897 | 25.60 | 25.32 | 2.58 |
| 971 | 25.66 | 25.37 | 2.74 |
| 1107 | 25.73 | 25.43 | 2.90 |
| 1420 | 25.87 | 25.59 | 3.19 |

## 5. RESULTS AND DISCUSSION

Table 2 lists the values of $k_c$, $k_v$ and $D$ at different temperatures for xenon in zeolite NaY. The Arrhenius plot of $k_c$ is shown in Figure 1. A straight line fitted to seven of the eleven points in the range 188 to 637 K is shown as a continuous line. It is seen that the points beyond 637 K do not lie on this line. This clearly suggests deviation from Arrhenius behaviour. A line fitted to the highest four of the eleven points in the range 897 to 1420 K is also shown by means of a broken line. These two fitted lines have different slopes. The activation energies are 3.02 and 5.07 kJ mol$^{-1}$ for the seven lowest and four highest temperatures, respectively. These results suggest that the rate of intercage diffusion exhibits higher activation energies at higher temperatures.

We shall now attempt to understand the reason for this behaviour. Earlier investigations [2] have shown that the predominant mechanism of intercage diffusion at lower temperatures is via the s.-m. diffusion mode. This is also known as creep diffusion [9–11]. This is essentially due to the negligible population of the sorbate near the cage centre. At higher temperatures, the population near the cage centre increases. Consequently, the mechanism by which the sorbates migrate from a given cage to a neighbouring cage occurs via the c.d. mechanism [1,3]. The potential energy surface near the cage centre and the interconnecting 12-ring window is shown schematically in Figure 2. It is seen that for the s.-m. diffusion, the barrier across the 12-ring window is positive. For the c.d. mode, the barrier across the 12-ring window is negative. With this background knowledge, it is now possible to provide an explanation for the observed behaviour, namely, the increase of activation energy associated with the rate of intercage diffusion $k_c$ with increase in temperature. At low temperature, when the s.-m. mode is the predominant mode of intercage diffusion, the activation energy corresponds to the barrier via this route. More precisely, the average activation energy is obtained from the expression

$$k(B) = k_0 \exp(-B/RT) \tag{4}$$

where $B$ is the barrier for a given trajectory. The rate $k = k(B)$ has to be integrated over all the trajectories. At higher temperatures, the predominant mode is the c.d. mode. For this mode the activation energy for diffusion across the 12-ring window is negative. However, the sorbate needs to be excited towards the cage centre before it can slide across to the neighbouring cage. In this case, the activation energy is the energy required to excite the sorbate from the vicinity of the inner surface of the cage to

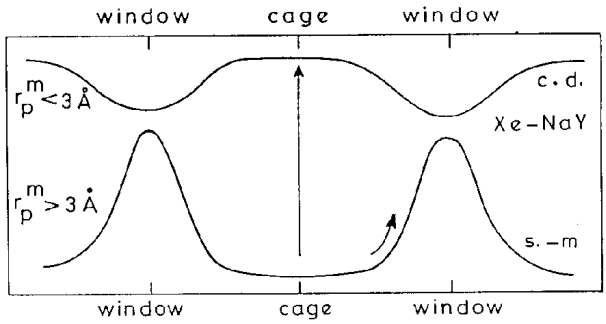


*Figure 2. Schematic illustration of the variation of potential energy for centralized ($r_p^m < 3$ Å) and surface-mediated ($r_p^m > 3$ Å) mode*

the region near the cage centre. This is larger than the activation energy required for intercage diffusion via the s.-m. mode. With an increase in temperature, the fraction of trajectories diffusing via the c.d. mode increases with a corresponding decrease in the fraction of trajectories diffusing via the s.-m. mode. This results in an increase in the activation energy with temperature for $k_c$. Some idea of the change in the activation energy can be obtained from Table 3. Here the activation energy is calculated by fitting only the first two highest temperature points. Then a third point immediately below these two temperatures is added and so on until all the eleven points are included in the fit.

This behaviour arises because of the fact that $k_c$ is predominantly determined by the nature of the potential energy surface near the region of the window. This is because of the definition of $k_c$ and the way $k_c$ is calculated. It has been pointed out that the rate has to be corrected for recrossings [12–14]. We have the rate of cage visits, $k_v$ which does not include any recrossings. A plot of ln $k_v$ against reciprocal temperature is shown in Figure 3a. It is seen that all the points fall on a straight line suggesting that the rate of cage visits obeys the Arrhenius relationship over the whole range of temperature. This is consistent with our earlier finding that the rate of cage visits depends on the long-time behaviour [3]. The recrossings account for a somewhat significant part of $k_c$ if the potential energy near the window is a minimum as is the case for argon in zeolite NaCaA [3]. Figure 3b shows the Arrhenius plot for $D$. All the points lie on a straight line suggesting again that the Arrhenius expression provides a valid

Table 3. Values of activation energy obtained from the slope of ln $k_c$ versus $1/T$ plot (see Figure 1) after a straight-line fit to several number of points starting from the highest to the lowest temperatures

| No. of points fitted | $E_a$ (kJ mol$^{-1}$) |
|---|---|
| 2 | 5.52 |
| 3 | 5.16 |
| 4 | 5.07 |
| 5 | 3.78 |
| 6 | 3.43 |
| 7 | 3.38 |
| 8 | 3.18 |
| 9 | 3.17 |
| 10 | 3.13 |
| 11 | 3.07 |

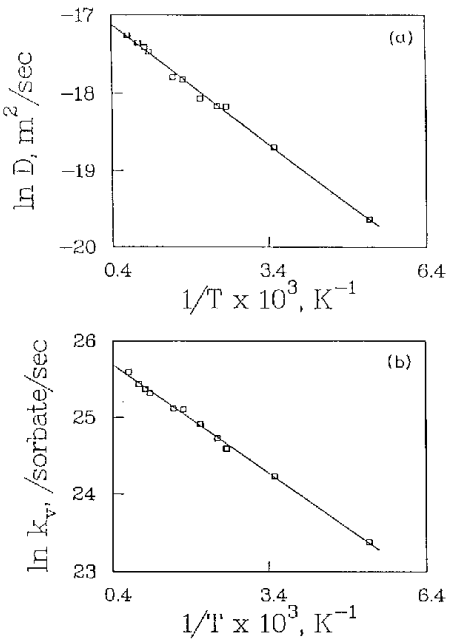


*Figure 3. Arrhenius plots of (a) the rate of cage visits, $k_v$ and (b) the diffusion coefficient, D.*

description of the diffusion coefficient over the whole range of temperatures investigated.

The above results confirm the earlier finding that $k_c$ is dependent on the short-time behaviour. This implies that $k_c$ is dependent on the nature of the local potential energy surface near the window. This is responsible for the non-Arrhenius behaviour of $k_c$. In contrast, the variation of $k_v$ and $D$ with temperature is found to be Arrhenius. This is consistent with the earlier suggestion that these properties are dependent on the long-time dynamics of the system and are independent of the nature of the local potential energy surface [3].

## REFERENCES


1. S. Yashonath and P. Santikary, *J. Phys. Chem.*, **97**, 3849 (1993).
2. S. Yashonath, *J. Phys. Chem.*, **95**, 5877 (1991).
3. S. Yashonath and P. Santikary, *J. Phys. Chem.*, **97**, 13778 (1993).
4. A. N. Fitch, H. Jobic and A. Renouprez, *J. Phys. Chem.*, **90**, 1311 (1986).
5. D. H. Olson, *J. Phys. Chem.*, **72**, 4366 (1968).
6. S. Yashonath, J. M. Thomas, A. K. Nowak and A. K. Cheetham, *Nature*, **331**, 601 (1988).
7. M. P. Allen and D. J. Tildesley, *Computer Simulation of Liquids*, Clarendon Press, Oxford, 1987.
8. A. V. Kiselev and P. Q. Du, *J. Chem. Soc. Faraday Trans. 2*, **77**, 1 (1981).
9. E. G. Derouane, *Chem. Phys. Lett.*, **142**, 200 (1987).
10. I. Derycke, J. P. Vigneron, Ph. Lambin, A. A. Lucas and E. G. Derouane, *J. Chem. Phys.*, **94**, 4620 (1991).
11. E. G. Derouane, J-M. Andrew and A. A. Lucas, *J. Catal.*, **110**, 58 (1988).
12. D. Chandler, *J. Chem. Phys.*, **68**, 2959 (1978).
13. J. A. Montgomery, D. Chandler and B. J. Berne, *J. Chem. Phys.*, **70**, 4056 (1979).
14. A. F. Voter and J. D. Doll, *J. Chem. Phys.*, **82**, 80 (1985).